Aalborg Universitet

Aalborg University

DENMARK

Glacial rock flour reduces the hydrophobicity of Greenlandic cultivated soils

Weber, Peter L.; Hermansen, Cecilie; Pesch, Charles; Moldrup, Per; Greve, Mogens H.; Blaesbjerg, Natasha H.; Romero, Gabriela Moreno; Arthur, Emmanuel; de Jonge, Lis Wollesen

Link to publication from Aalborg University

ORIGINAL ARTICLE

Soil Physics & Hydrology

Soil Science Society of America Journal

Glacial rock flour reduces the hydrophobicity of Greenlandic cultivated soils

Peter L. Weber[1] | **Cecilie Hermansen**[1] | **Charles Pesch**[1] | **Per Moldrup**[2] | **Mogens H. Greve**[1] | **Natasha H. Blaesbjerg**[2,3] | **Gabriela Moreno Romero**[1] | **Emmanuel Arthur**[1] | **Lis Wollesen de Jonge**[1]

[1]Department of Agroecology, Faculty of Technical Sciences, Aarhus University, Denmark

[2]Department of the Built Environment, Faculty of Engineering and Science, Aalborg University, Denmark

[3]Tasmanian Institute of Agriculture, University of Tasmania, Hobart, Australia

Correspondence
Peter L. Weber, Department of Agroecology, Faculty of Technical Sciences, Aarhus University, Blichers Allé 20, DK-8830 Tjele, Denmark.
Email: plw@agro.au.dk

Assigned to Associate Editor XiaoYan Li.

Abstract

Soil water repellency (WR) is ubiquitous across Greenlandic cultivated fields, which may constrain agricultural production. Fine-grained glacial rock flour (GRF) is available in the surrounding landscape, which could serve as a soil amendment. We tested whether the application of GRF (rates of 0, 50, 100, 300, and 500 ton ha^{-1}) reduced the WR across two field trials in South Greenland. The field trials, Upernaviarsuk (UP) and South Igaliku (SI), differed in clay (UP: 0.05–0.11 kg kg^{-1}; SI: 0.03–0.05 kg kg^{-1}) and organic carbon (OC) contents (UP: 0.04–0.13 kg kg^{-1}; SI: 0.01–0.03 kg kg^{-1}). We measured WR across gravimetric water contents (W) from oven-dry to the W where WR ceased (W$_{NON}$) to obtain whole WR-W curves. Most soils became hydrophilic around air-dry conditions at application rates of ≥300 ton ha^{-1}, likely due to increased clay:OC ratios. Application rates of ≥300 ton ha^{-1} generally reduced the trapezoidal integrated area of the WR-W curve (WR$_{AREA}$), W$_{NON}$, and WR after heat treatments at 105°C (WR$_{105}$) and 60°C (WR$_{60}$). The WR$_{105}$ was significantly reduced in both fields at 500 ton ha^{-1}, while WR$_{60}$ was significantly reduced in UP at application rates of ≥300 ton ha^{-1}. The GRF effects were masked by texture and OC variations. Normalizing WR$_{AREA}$ to the water vapor sorption isotherms (utilizing the Campbell-Shiozawa model) revealed that GRF consistently reduced the normalized WR$_{AREA}$. The SI field showed the largest reduction in the normalized WR$_{AREA}$, likely due to its lower OC and clay contents. Thus, GRF could reduce WR across two Greenlandic field trials.

1 | INTRODUCTION

Soil water repellency (WR) originates from the presence of hydrophobic organic compounds that cover the soil mineral fraction (Bisdom et al., 1993). The hydrophobic compounds may originate from, for example, decomposing plant tissues, root exudates, fungal hyphae, plant-derived waxes, as well as microbially-derived compounds and necromass (Doerr et al., 2000; Hallet, 2008). Further, abiotic processes, for example, forest fires, may also cause severe hydrophobic coatings within the subsoil (Doerr et al., 2000; Wallis & Horne, 1992).

Abbreviations: GRF, glacial rock flour; MED, molarity of an ethanol droplet; OC, organic carbon; SI, South Igaliku; UP, Upernaviarsuk; W, gravimetric water content; WR, soil water repellency.

The hydrophobic organic compounds reduce the surface tension of the soil particles, which may result in resistance to wetting at time scales ranging from seconds to weeks (Doerr et al., 2000; King, 1981). Several techniques have been used to determine the WR of soils, with two of the most popular methods being the water droplet penetration time (WDPT) and the molarity of an ethanol droplet (MED) test (Hallet, 2008; King, 1981). The WDPT reflects the persistence of WR by measuring the infiltration time of a water droplet, while the MED test measures the degree of WR by modulating the surface tension of the infiltrating droplet (King, 1981; Roy & McGill, 2002).

The degree of WR is dynamic since amphibolic compounds can reorientate and expose either hydrophobic or hydrophilic ends according to the gravimetric water content (W) (Doerr et al., 2000). The WR-W curve of water repellent soils can be either unimodal or bimodal (de Jonge et al., 1999). The unimodal curves are characterized by a single peak in WR that typically occurs between air-dry conditions and the permanent wilting point (Kawamoto et al., 2007; Kercheva et al., 2021; King, 1981; Wijewardana et al., 2016), while bimodal curves exhibit an additional peak close to oven-dry conditions (de Jonge et al., 1999). Water repellent soils become hydrophilic when the water content exceeds the critical water content (W_{NON}), which can vary significantly depending, inter alia, on the texture, organic carbon (OC) content, and clay content (de Jonge et al., 1999; Hermansen et al., 2019; Weber et al., 2021). The W_{NON} has generally been reported to occur at or around pF 3, where $pF = \log[\psi$, in cm $H_2O]$, but W_{NON} has been reported to occur at less than pF 2 (Kawamoto et al., 2007; Kercheva et al., 2021; Wijewardana et al., 2016). Thus, soils can be hydrophobic across relatively large ranges in W and even at water contents above field capacity.

The nonlinear WR-W curve is often parameterized using the total WR (i.e., the trapezoidal integrated area of the WR-W curve; WR_{AREA}) and W_{NON} (de Jonge et al., 1999, 2007; Kawamoto et al., 2007; Regalado et al., 2008). Further, the severity of WR after heat pre-treatments at 60°C (WR_{60}) and 105°C (WR_{105}) can also be used as indices for WR characterization (de Jonge et al., 1999).

While the majority of the studies on WR originate from semiarid and Mediterranean climates, it is becoming increasingly evident that WR also occurs in wetter and colder climates (Doerr et al., 2000; Fu et al., 2021; Hermansen et al., 2019; Seaton et al., 2019). A recent study on soils collected across 23 pasture and cultivated fields in South Greenland revealed that 99% of these soils were water repellent, with 98% of the soils being capable of reaching an extremely high degree of WR (surface tension <40.9 mN m^{-1}) (Blaesbjerg et al., 2022; Weber et al., 2021). The high prevalence of WR in these subarctic soils was ascribed to a combination of coarse particle size distribution and high OC content (Weber et al., 2021). Further, Weber et al. (2021) found that both

Core Ideas

- Applying fine-grained glacial rock flour (GRF) may alleviate highly hydrophobic subarctic soils.
- Moisture-dependent hydrophobicity was assessed in two field trials in South Greenland.
- Parameters evaluated included both total area under the hydrophobicity curve and single-point values.
- Hydrophobicity was reduced at GRF applications ≥300 ton ha^{-1}, particularly in the less clayey field.
- Normalizing the level of hydrophobicity to the level of water retention enabled comparisons between soils.

WR_{AREA} was strongly governed by the OC content ($r^2 = 0.91$) and that both clay and OC content contributed to the W_{NON} ($r^2_{adj} = 0.92$).

Soil water repellency can constrain agricultural production (Müller et al., 2010; Roper et al., 2015) by increasing surface runoff and erosion, reducing rain- or irrigation-water infiltration, and reducing nutrient availability (Doerr et al., 2000; Roper et al., 2015). Given the high prevalence of WR in Greenland, it would be beneficial to ameliorate WR. It is possible to alleviate WR by different methods. Among these are cultivation, clay amendment, application of soil wetting agents, and irrigation (Müller & Deurer, 2011; Wallis & Horne, 1992). While the mechanism by which clay amendment reduces the WR is still unclear, the effect has been attributed to the masking of hydrophobic surfaces by clay minerals, which has a large and negatively charged specific surface area (Dlapa et al., 2004; Müller & Deurer, 2011). Nevertheless, clay amendment is often used as an indirect amelioration technique for hydrophobic soils in Australia (Müller & Deurer, 2011). Further, studies have shown that clay amendment is an effective strategy for WR amelioration in both naturally hydrophobic sandy soils and "model" soils, where initially hydrophilic sands are made artificially water repellent by adding organic hydrophobic compounds, for example, cetyl alcohol, stearic acid, or organic extracts (Ma'shum et al., 1989; McKissock et al., 2002; Diamantis et al., 2017; Ward & Oades, 1993). Clay amendment is only economically feasible if the clay is readily available from a local source (Hallet, 2008; Müller & Deurer, 2011). Pesch et al. (2022) reported that glacial fjords in South Greenland contain vast amounts of glacial rock flour (GRF); a glacially derived mineral material with a high content of clay- and silt-sized particles that have a specific surface area corresponding to soils dominated by kaolinite clay (Pesch et al., 2022). Thus, it would be

beneficial if the nearby glacial rock flour deposits could be applied to Greenlandic agricultural soils to ameliorate WR.

In general, there is broad acceptance that kaolinite clay is useful for WR amelioration. In contrast, studies have reported both successful and less successful results for illite and montmorillonite clays. The effectiveness of kaolinite clay in reducing WR as compared to montmorillonite clay might be attributed to the comparably high dispersibility of kaolinite clays, which can facilitate a readily, long-term, and even distribution of the clay mineral over hydrophobic grain surfaces (Cann, 2000; Ma'shum et al., 1989; Ward & Oades, 1993). The effect of clay amendment on WR is not enabled until the soil has been through one or more wetting and drying cycles since wetting facilitates the distribution of clay around soil particles, and drying facilitates the masking of hydrophobic compounds (McKissock et al., 2002; Ward & Oades, 1993).

Few studies exist on the effect of GRF as a soil amendment since the idea is relatively new, and no studies have investigated the potential of GRF to ameliorate the WR of Greenlandic agricultural soils. Presently, the GRF amendment investigations have focused primarily on nutrient supply, crop yield, and the plant available water (Pesch et al., 2022; Sukstorf et al., 2020). If GRF behaves somewhat similarly to kaolinite clay, applying GRF could become a viable option for Greenlandic farmers to reduce the WR of their coarse-grained soils.

Based on two field trials located in Southern Greenland, the overall aim of this paper was to assess changes in WR 1–2 years after field application of GRF in different concentrations (0, 50, 100, 300, and 500 ton ha^{-1}). Assessing the effect of GRF on WR 1–2 years after application allows the soil to undergo several wetting and drying cycles, which can provide a realistic assessment of the efficacy of GRF for WR amelioration in Greenland. We hypothesized that the GRF application would result in marked reductions of the WR, which would be reflected in the degree of WR after heat pre-treatments (WR$_{60}$ and WR$_{105}$) and a decrease in both WR$_{AREA}$ and W$_{NON}$. To achieve the overall aim, the objectives were to test if GRF application affects the WR parameters (WR$_{AREA}$, W$_{NON}$, WR$_{60}$, and WR$_{105}$) and whether GRF application affects the relationship between the WR parameters and OC.

2 | MATERIALS AND METHODS

2.1 | Field trials

Two field trials were established in Upernaviarsuk (UP, 60°44′57.3′′ N, 45°53′24.4′′W) and South Igaliku (SI, 60°53′15.2′′ N, 45°16′37.1″ W) in 2018 and 2019, respectively (Figure 1). Despite that the agricultural production in Greenland is very limited, the agricultural history and present agricultural production is well described (e.g., Caviezel et al., 2017; Jacobsen, 1987; Weber et al., 2020).

A large climatic gradient characterizes the study area due to the influences of the polar air from the inland ice cap and the oceanic air mass from the Davis Strait. Consequently, the climate changes from oceanic climate in the outer parts of the fjords (UP) to sub-oceanic/subarctic climate in the middle parts of the fjords (SI) (Jacobsen, 1987). Two weather stations exist within the study area, one near UP and one in Narsarsuaq (Figure 3), which are situated in the outer and inner parts of the fjords, respectively. For the 1981–2010 period, the mean annual precipitation ranged from 986.5 mm near UP to 650.7 mm in Narsarsuaq, and the mean annual temperature was 0.8 and 1.1°C, respectively (Cappelen, 2021). The average number of growing days ranges from approximately 100 days in the outer fjord to approximately 145 days in Narsarsuaq (Christensen et al., 2016).

The UP soil was classified as a Leptic Cambisol (IUSS Working Group WRB, 2014) with a loamy sand texture that developed on colluvium originating from granodioritic gneiss and granites of the Julianehåb batholith (Kokfelt et al., 2019) since the last deglaciation approximately 10 ka BP (Bennike et al., 2002). The SI soil was classified as a Brunic Arenosol (IUSS Working Group WRB, 2014) with a loamy sand texture that developed on top of aeolian and fluvial sediments originating from the surrounding bedrock, including hornblende bearing diorite and gabbro and olivine-bearing syenite (Kokfelt et al., 2019). Both fields have been cultivated and used for hay production with perennial grasses for >50 years. Before the experiment, both fields had been vegetated by similar commercial grass mixtures, which primarily consisted of timothy (*Phleum pratense* L.), colonial bentgrass (*Agrostis tenuis* L.), Kentucky bluegrass (*Poa pratensis* L.), Perennial ryegrass (*Lolium perenne* L.), and red fescue (*Festuca rubra* L.). It was estimated that both fields produced an average annual yield of 4 tons dry matter per hactare, and neither of the fields had been tilled within the last 3 years.

The UP-field trial was established first as part of a feasibility study at the agricultural research station and agricultural school in UP immediately after the harvest in mid-August 2018. The trial was arranged in a randomized block design with five application rates of glacial rock flour, 0 (control), 50, 100, 300, and 500 ton ha^{-1}, which were replicated ($n = 4$), yielding a total of 20 field plots. Each plot was 3×3 m^2, and the spacing between each plot was 3 m along the tillage direction and 2 m perpendicular to the tillage direction. The GRF was manually disaggregated, applied evenly on the soil surface, and incorporated thoroughly into the upper 15 cm of the A horizon using a disc harrow. The field was sown with the commercial grass mixture consisting of 85% timothy (*Phleum pratense* L.), 10% colonial bentgrass (*Agrostis tenuis* L.), 3% Kentucky bluegrass (*Poa pratensis* L.), and 2% Dutch clover
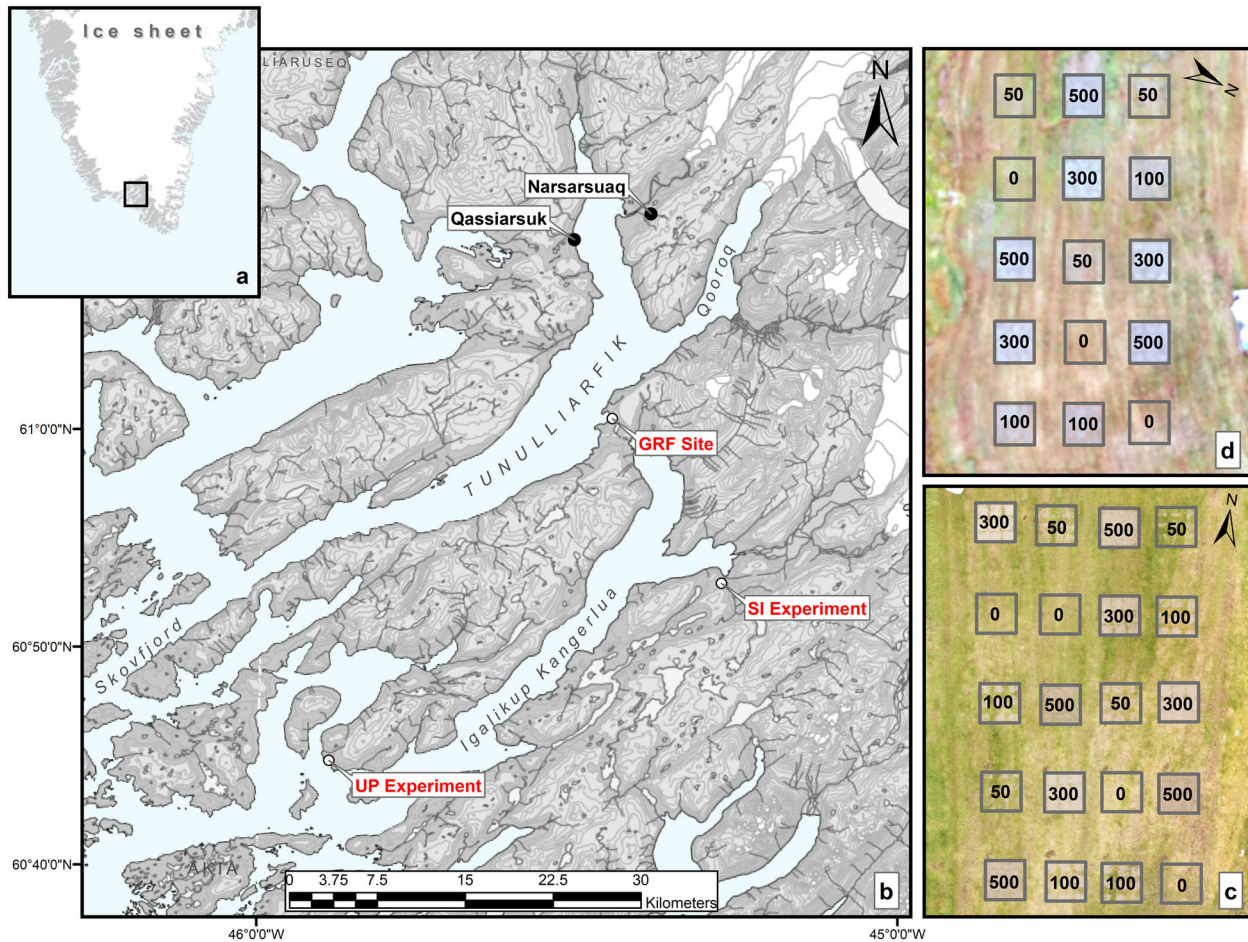
FIGURE 1 (a) Map showing the wider location of the study area in Greenland and (b) the location of the glacial rock flour (GRF) site and the experimental sites in Upernaviarsuk (UP) and South Igaliku (SI). Drone images of the UP (c) and SI (d) field trials immediately before the incorporation of the glacial rock flour (GRF). The plot extent is highlighted with grey squares, and the numbers within each plot denote the application rate of GRF in ton ha^{-1}. GIS maps by Asiaq Greenland Survey (2022).

(*Trifolium repens* L.). Commercial NPK fertilizer (17:7:14) was applied in early spring every year, corresponding to an application rate of approximately 110 kg N ha^{-1}, 45 kg P ha^{-1}, and 91 kg K ha^{-1}.

The SI field trial was established in 2019, almost identical to the UP trial, with the only difference being a reduced number of replications ($n = 3$, total plots = 15) due to the size of the field.

The GRF used in both experiments originated from a large (approximately 1,400,000 m^3) local deposit in Ataanasit (AT, 61°00′47.8″ N, 45°27′04.5″ W), which consists of raised marine sediments originating from the surrounding glacial outwash streams (Pesch et al., 2022). The deposit is one among many in the area that has been exposed due to isostatic rebound after the last deglaciation, approximately 10 ka BP (Bennike et al., 2002). The GRF is non-saline, consisting of 0.44 kg kg^{-1} fine particles (≤ 20 μm) with a mineralogical composition dominated by feldspars (73%) and quartz (15%), with traces of amphiboles (6%) and micas (6%). A detailed physical characterization of the used GRF (AT) and

other GRFs from southwest Greenland can be found in Pesch et al. (2022).

2.2 | Soil sampling and analyses

Bulk soil was sampled from each plot before applying GRF to serve as a secondary control for each plot while also establishing a baseline in WR across the two fields. In both field trials, the post-treatment soil sampling was performed immediately after harvest in mid-August 2020. Thus, the GRF was incorporated into the soil for 2 years in the UP trial and one year in the SI trial at the post-treatment sampling. During each soil sampling, approximately 2 kg of bulk soil was excavated in the A horizon immediately below the turf layer resulting in a total soil depth of approximately 5–10 cm. A 2 kg GRF sample was also acquired by mixing 12 representative subsamples from the excavated material prior to the application in the field. Before further analyses, all bulk samples were stored at 2°C and subsequently air-dried at 20°C.
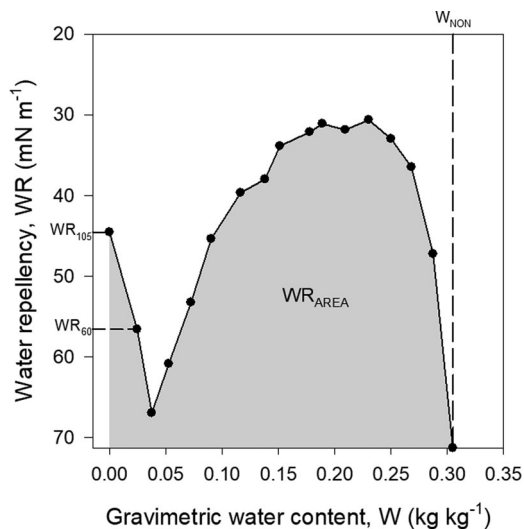
FIGURE 2 Conceptual figure showing the soil water repellency (WR) as a function of gravimetric water content (W) and the four parameters derived from the WR-W curve. The WR after oven-drying at 105 and 60°C is denoted WR_{105} and WR_{60}, respectively, and WR_{AREA} is the trapezoidal integrated area of the WR-W curve. The W above which the soil sample is hydrophilic is denoted W_{NON}. WR-W curve, curve of water repellent soils.

The particle size distribution was determined by a combination of wet-sieving and the pipette method after organic matter removal (Gee & Or, 2002). A total of five particle sizes were determined following an extended version of the ISSS system (Table 1). Additionally, the USDA textural classes of the soils were obtained by estimating the 2–50 μm fraction using log-linear interpolation of the cumulative grain-size distributions. Total OC was measured by dry combustion with an ELTRA Helios C-Analyzer (ELTRA GmbH). The OC was set equal to the total carbon as all samples tested negative for calcium carbonates using a 10% HCl solution.

2.3 | Soil water repellency

The molarity of an ethanol droplet test (MED; de Jonge et al., 1999; King, 1981; Roy & McGill, 2002) was used to determine the WR of each soil. The WR was measured across a range in W to account for the entire soil water repellency characteristic, that is, the WR-W curve (Figure 2). Two oven-drying pre-treatments were used to account for the dry range (i.e., W below air-dry) of the WR-W curve while also serving as standardized WR indices. The first oven-drying pre-treatment consisted of oven-drying the soil at 105°C for 24 h and measuring the WR directly after cooling in a desiccator for 2 h (WR_{105}). The second and oven-drying pre-treatment consisted of oven-drying the soil at 60°C for 24 h followed by a 48 h equilibration at 20°C in a climate-controlled laboratory (WR_{60}). Further, the WR was measured

TABLE 1 Summary of the physical properties of the soils from the two field trials, Upernaviarsuk (UP) and South Igaliku (SI), and the glacial rock flour (GRF), prior to the GRF application.

Field	N	Statistics	Clay (kg kg^{-1})	Fine silt (kg kg^{-1})	Coarse silt (kg kg^{-1})	Fine sand (kg kg^{-1})	Coarse sand (kg kg^{-1})	OC (kg kg^{-1})	WR$_{AREA}$ (mN m^{-1} kg kg^{-1})	W$_{NON}$ (kg kg^{-1})	WR$_{105}$ (mN m^{-1})	WR$_{60}$ (mN m^{-1})	$-\alpha^{-1}$
UP	20	Mean	0.080	0.077	0.162	0.250	0.430	0.082	8.13	0.307	44.36	58.93	0.036
		Min	0.047	0.063	0.129	0.155	0.263	0.042	4.65	0.178	41.54	51.82	0.021
		Max	0.111	0.095	0.226	0.381	0.553	0.125	13.14	0.488	48.24	71.27	0.047
		Std	0.018	0.008	0.023	0.054	0.073	0.022	2.30	0.080	1.69	5.45	0.008
SI	15	Mean	0.039	0.051	0.198	0.577	0.136	0.019	2.13	0.087	58.76	66.23	0.010
		Min	0.026	0.029	0.164	0.407	0.083	0.012	0.88	0.046	48.24	47.21	0.006
		Max	0.050	0.078	0.228	0.655	0.275	0.028	3.30	0.121	71.27	71.27	0.015
		Std	0.007	0.014	0.019	0.068	0.049	0.006	0.74	0.024	5.68	6.99	0.003
GRF	1	–	0.207	0.235	0.153	0.204	0.202	0.000	0.00	–	71.27	71.27	0.012

Note: Depth of soils: clay, <2 μm; fine silt, 2–20 μm; coarse silt, 20–60 μm; fine sand 60–200 μm; coarse sand, 0.2–2 mm.

Abbreviations: $-\alpha^{-1}$, inverse of the pF-W slope; Max, maximum; Min, minimum; OC, organic carbon; Std, standard deviation; W_{NON}, critical water content; WR_{60}, soil water repellency after 60°C; WR_{105}, soil water repellency after 105°C; WR_{AREA}, trapezoidal area of the soil water repellency (WR)–water content (W) curve.

on a series of rewetted soil samples where the W ranged between air-dry and the W_{NON} for each soil (Figure 2). The rewetted soil samples were prepared by mixing 20 g of air-dry soil with tap water in Ziploc bags and equilibrating the samples in a 4°C dark room for 3 weeks. The target water content for each series was calculated based on the expected W_{NON}, which was calculated using the OC-based PTF for W_{NON} created by Weber et al. (2021) for 145 Greenlandic agricultural topsoils.

The MED measurement was performed using dilution series of ethanol and deionized water with ethanol concentrations ranging between 0.00 and 0.80 m³ m⁻³ in 0.01 m³ m⁻³ increments. First, pretreated soil samples were quickly placed in small plastic cups, and the soil surface was smoothed and leveled with a knife. Thereafter, the samples were immediately subjected to a normal stress of 60.9 Nm⁻² for 2 min using a tight-fitting press that minimized water evaporation prior to the MED measurement. Droplets of 60 μL ethanol solution were left on the soil surface to infiltrate, and the WR, that is, surface tension (mN m⁻¹), of the soil sample was derived from the highest ethanol concentration that did not infiltrate within 5 s as outlined by Roy and McGill (2002). The actual W at each WR measurement was obtained by oven-drying a subsample of the pretreated soil at 105°C for 24 h. The total degree of WR for each soil was calculated using the trapezoidal integrated area under the WR-W curve (WR_{AREA}). A conceptual figure of a typical WR-W curve and the derived WR parameters is shown in Figure 2.

2.4 | Measurement of water vapor sorption

Water vapor sorption isotherms at 25°C were measured on all air-dry samples using an automated vapor sorption analyzer (METER Group Inc.). A full adsorption-desorption loop was measured in the relative humidity range of 3%–93% with a resolution of 2%. The endpoint water content was subsequently measured by oven-drying at 105°C for 24 h. An in-depth description and discussion of the procedure can be found in Arthur et al. (2014).

The water vapor sorption isotherms were subsequently converted to pF-based soil water retention curves (pF-W relationship) using the Kelvin equation (Equation 1) and the Schofield equation (Equation 2) as follows:

$$\psi = \frac{RT \ln(RH)}{M_{H2O} g} \tag{1}$$

$$pF = \log_{10}(|\psi|) \tag{2}$$

where ψ is the soil water matric potential (cm H_2O), R is the ideal gas constant (8.31 J mol⁻¹ K⁻¹), T is the temperature (kelvin), M_{H2O} is the molecular mass of H_2O (0.018 kg mol⁻¹), g is the gravitational acceleration constant (9.807 m s⁻²), and RH is the relative humidity (%).

2.4.1 | Normalization of the SWR_{AREA} to the soil water retention

The simple semi-logarithmic Campbell-Shiozawa model (Campbell & Shiozawa, 1992) was utilized as a soil water retention model to normalize the measured SWR_{AREA} to the dry-region soil water retention and thereby enable direct comparison across the treatments and field trials.

To minimize the hysteretic effects in the terminal ends of the water vapor sorption isotherms (Figure 3), the Campbell-Shiozawa model (Equation 3) was fitted to the linear part of the desorption isotherm between pF 6.35 and 5.69, corresponding to a relative humidity between 20 and 70% as follows:

$$pF = pF_0 + \alpha W \tag{3}$$

where W is the gravimetric water content (kg kg⁻¹), and the fitting parameters pF_0 and α represent the pF at zero water content and the dimensionless slope of the pF-W relationship, respectively.

The normalization was performed by dividing the SWR_{AREA} with the inverse of the negative Campbell-Shiozawa model slope ($-\alpha^{-1}$). This operation was motivated by the findings of Weber et al. (2020), who found that both SWR_{AREA} and W_{NON} scaled linearly with $-\alpha^{-1}$ in Greenlandic agricultural soils. Thus, it should be possible to directly compare soils with different OC and clay content when normalizing the SWR_{AREA} with the dry-region soil water retention ($-\alpha^{-1}$). The rationale behind this approach is further discussed in Section 3.4.

2.5 | Statistical analysis

The differences between post-treatment groups were evaluated with a one-way analysis of variance (ANOVA) coupled with a pairwise multiple comparison using the Holm-Sidak method (Holm, 1979). Differences between the pre-sampling and post-treatment results were analyzed for each application rate using a paired t-test. The variables were evaluated for normality and equality of group variance using the Shapiro-Wilk test and Brown-Forsythe test, respectively (Brown & Forsythe, 1974; Shapiro & Wilk, 1965). All statistical analyses were performed in Sigma Plot 14.5 (Systat Software, Inc.). Linear correlations between the WR parameters and OC were evaluated using the coefficient of determination (R^2) and Pearson's correlation coefficient (r).
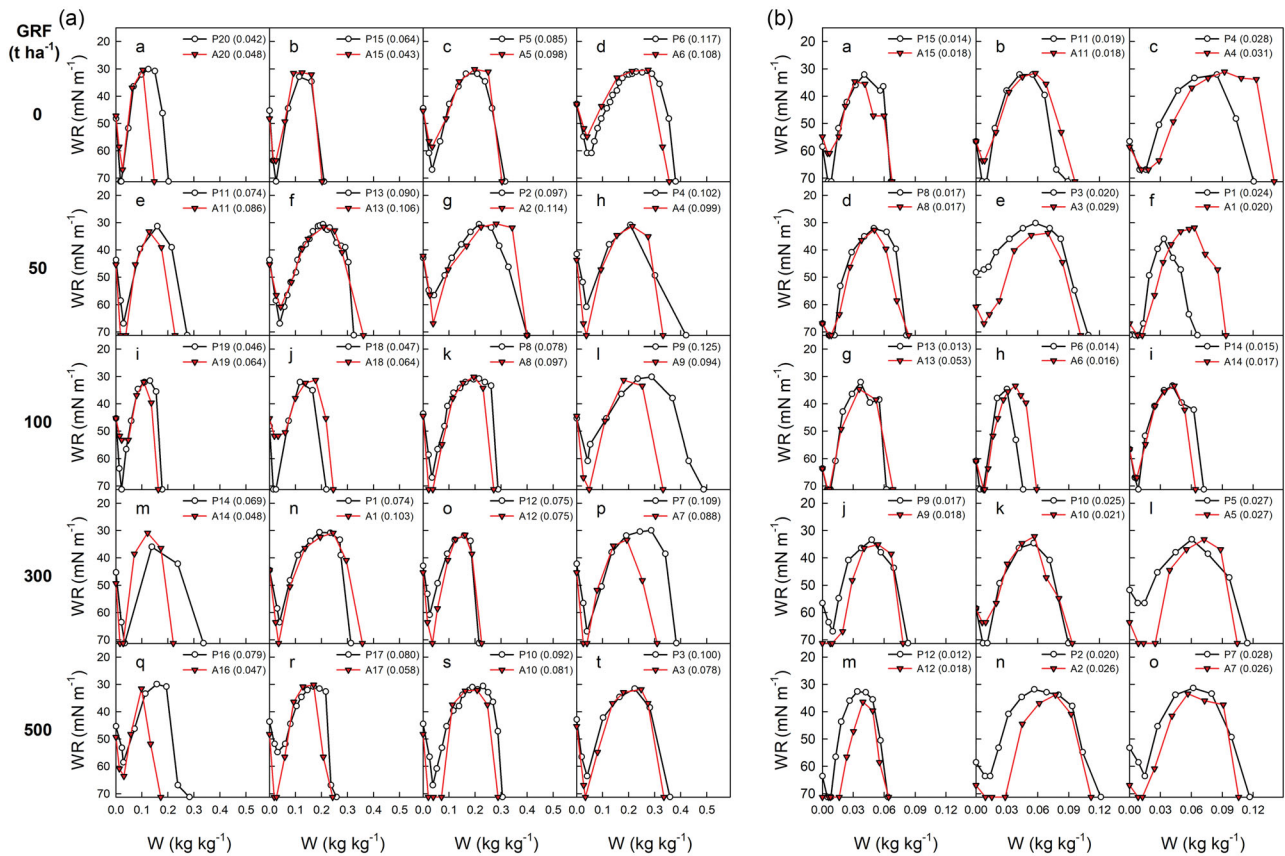
FIGURE 3 Soil water repellency as a function of gravimetric water content (W) for the UP field (a) and the SI field (b). Black curves with open white circles denote the results from the pre-sampling (P1–20) before application of glacial rock flour (GRF), and the red lines with red open triangles denote the post-treatment results, that is, after application of GRF (A1–15). Each row represents an application rate of GRF, and the rows are arranged according to their organic carbon (OC) content (brackets) at the time of pre-sampling (kg kg^{-1}). SI, South Igaliku; UP, Upernaviarsuk.

3 | RESULTS AND DISCUSSION

3.1 | Particle size distribution and organic carbon

All SI plots and 18 of the UP plots were classified as loamy sand, while two UP plots were classified as sand and sandy loam according to Soil Survey Staff (1999). However, marked differences in the particle size distribution were apparent between the two fields despite their comparable textural classes (Table 1), with the SI field consisting predominately of fine sand (0.407–0.655 kg kg^{-1}) and the UP field exhibiting a high content of coarse sand (0.263–0.430 kg kg^{-1}). Additionally, the clay content was approximately twice as high in the UP field (0.047–0.111 kg kg^{-1}) compared to the SI field (0.026–0.050 kg kg^{-1}).

The average OC content was approximately four times higher in the UP field (0.082 kg kg^{-1}) than in the SI field (0.019 kg kg^{-1}). Further, the OC also exhibited a large degree of variation in both fields, which was evident from the OC exhibiting a coefficient of variation of 27% and 32% for UP in the UP and SI fields, respectively.

3.2 | Effect of GRF on WR-W curves and the severity of WR

The WR-W curves of both the UP and SI fields were characterized by bimodal curve shapes (Figure 3), with the local minimum in WR located around water contents corresponding to air-dry conditions. This general behavior was similar to WR-W curves obtained from grass-based agricultural systems by Weber et al. (2021) and Hermansen et al. (2019), who used the same methodology to investigate large datasets from Greenland and New Zealand, respectively. When comparing the WR-W curves of the pre-GRF with the post-GRF control samples (0 ton ha^{-1}), the curves looked similar with two exceptions (Figure 3a(a),b(c)). The SWR-W curve in Figure 3a(a) obtained a higher W_{NON} for pre-GRF, and the SWR-W curve in Figure 3b(c) obtained a higher W_{NON} for the post-GRF treatment sample. The most prominent deviations between pre-GRF and post-GRF samples occurred for soils that exhibited markedly different OC content (e.g., Figure 3a(l),a(q)), where higher OC contents resulted in a general shift along the x-axis. This phenomenon was also noted by Hermansen et al. (2019), who found that OC directly

governed both the W_{NON} ($R^2 = 0.68$) and WR_{AREA} ($R^2 = 0.68$) across several soil types.

At the application rates of 50 and 100 ton ha^{-1}, the effect of GRF was not clear from the visual comparison of the WR-W curves. However, at application rates of 300 and 500 ton ha^{-1}, it was possible to identify changes in WR after GRF application visually. The samples became hydrophilic under air-dry conditions at an application rate of 300 ton ha^{-1} (except for one sample from the SI field; Figure 3b(k)). The same trend was valid for the application rate of 500 ton ha^{-1}, where the samples became hydrophilic at air-dry conditions (except for one sample from the UP field; Figure 3a(q). Thus, WR disappeared for six out of seven samples at air-dry conditions after GRF application of 300 and 500 ton ha^{-1}, respectively. For the WR_{60} measurement, all samples from the SI field became hydrophilic at the 500 ton ha^{-1} application rate. By visually interpreting the area underneath the curves at GRF application rates of 300 and 500 ton ha^{-1}, it was also possible to see that WR_{AREA} decreased for some field plots (e.g., Figure 3a(p,q),b(n)).

In the UP field, the WR_{AREA} and W_{NON} of post-GRF samples were lower than the measurements for the pre-GRF samples for all application rates (0, 50, 100, 300, and 500 ton ha^{-1}) (Figure 4a,b). In the SI field, the WR_{AREA} and W_{NON} of the post-GRF control samples (0 ton ha^{-1}) reached a higher level than the pre-GRF control samples (Figure 4e,f), indicating a general increase in both WR_{AREA} and W_{NON} between the sampling years. Based on the soil composition, it was not possible to explain the slightly diverging WR behavior of the pre-GRF and post-GRF control samples across the two field sites (including the differences seen in Figure 3a(a),b(c)). The slightly diverging WR behavior could likely result from measurement uncertainty and differences in, for example, pre-GRF sampling year, local climate, and time since tillage. Nevertheless, the observed differences between pre-GRF and post-GRF control samples were not statistically significant.

In both fields, the WR_{AREA} and W_{NON} of the post-GRF soils were consistently reduced compared to the pre-GRF sampling at the 300 and 500 ton ha^{-1} application rates. The ANOVA found no significant differences ($p < 0.05$) in WR_{AREA} and W_{NON} across the post-treatment levels. The paired t-test found no significant differences between the pre- and post-treatment values at each treatment level. However, the lack of statistical significance could partly be a result of relatively high variations in OC content observed at both the field- and plot-level (see brackets in Figure 3).

For the WR_{60} and WR_{105} measurements, the trends between the WR levels obtained during the pre-GRF and post-GRF sampling campaigns were not clear for GRF application rates of 0, 50, and 100 ton ha^{-1} (Figure 4c,d,g,h). However, the degree of WR at WR_{60} and WR_{105} were markedly lower during the post-GRF campaign than the pre-GRF campaign for the UP field at application rates of 300 and 500

ton ha^{-1}, which is represented by lower values in Figure 4 (note the modified x-axes). The paired t-test showed a significant ($p < 0.05$) reduction in WR_{105} between pre- and post-treatment for the highest application rate in both fields. Further, the ANOVA and Holm-Sidak test showed a significant difference in WR_{105} between post-treatment levels, with the 500 ton ha^{-1} being significantly ($p < 0.05$) different from the control (0 ton ha^{-1}).

The WR_{60} was significantly lower during the post-GRF sampling than the pre-GRF sampling for the UP field at application rates of 300 and 500 ton ha^{-1}. Although the reduction in WR_{60} was not significant in the SI field, the WR_{60} measurements after application of 500 ton ha^{-1} GRF showed that the soils became hydrophilic.

The fact that the largest effect of GRF was observed on WR_{105} and WR_{60} agrees well with the previous findings by Weber et al. (2021). They found that both WR_{105} and WR_{60} decreased with increasing clay:OC ratios across 145 Greenlandic soils. They further reported that the soils became hydrophilic at both pre-treatments when the clay:OC ratio was larger than two.

Different application rates of clay have been used throughout the literature for WR remediation. For example, Cann (2000) applied clay at rates of 0, 50, 100, and 150 ton ha^{-1} across an experimental site in Australia and obtained the highest reduction in WR for the application rate of 150 ton ha^{-1}. Further, Diamantis et al. (2017) applied kaolinite clayey soil onto water repellent sandy soil under olive trees at a rate of 10 ton ha^{-1} in both dry and wet form, and the wet application of clay immediately reduced WR by 74%. The study by McKissock et al. (2002) applied kaolinite and smectite clay at rates between 0%, 0.2%, 0.4%, 0.8%, and 1.6% by weight, respectively. In that study, they found a logarithmic relationship between the severity of the WR and the amount of clay added to the soil.

3.3 | Effect of GRF on the relationship between WR and OC

For both the UP and SI fields, WR_{AREA} ($R^2 = 0.87$ and 0.62, respectively) and W_{NON} ($R^2 = 0.62$ and 0.73, respectively) correlated significantly ($p < 0.001$) and linearly to OC content for the pre-GRF sampling (Figure 5a,e). The linear relationships were stronger for the UP field, possibly due to the wider range in OC content compared to the SI field. The WR_{105} and WR_{60} from the pre-GRF sampling also exhibited significant and linear correlations to OC content (Figure 5c,d,g), with the exception of WR_{60} in the SI field, which was a result of several samples being hydrophilic at WR_{60}.

The WR_{AREA} measurements of the UP control samples were distributed around the regression line, indicating that the relation between WR_{AREA} and OC content was comparable to
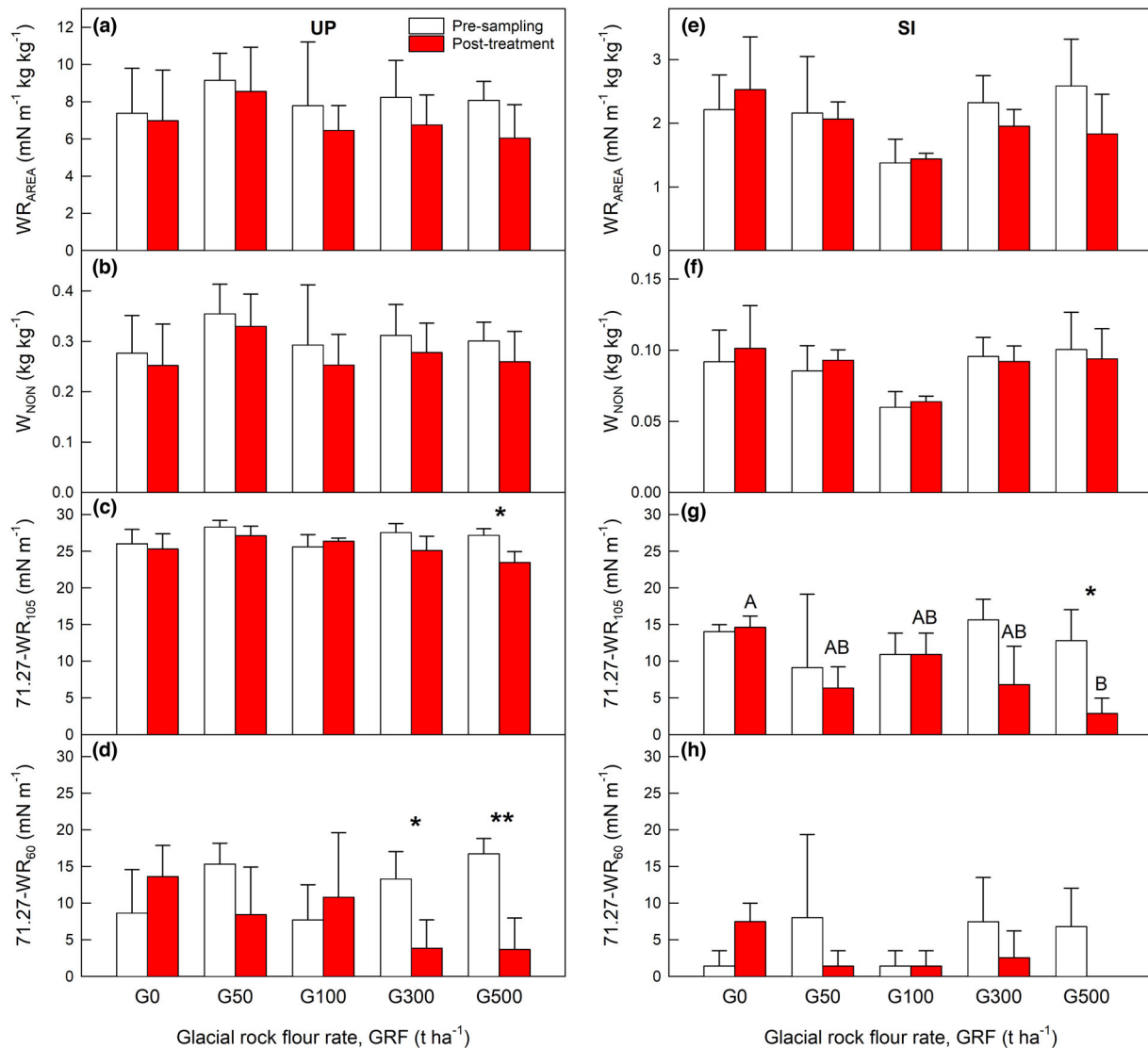
FIGURE 4 Bar charts of the trapezoidal integrated area of the WR-W curve (WR_{AREA}; a), the critical water content (W_{NON}; b), the degree of soil water repellency after 105˚C heat treatment (WR_{105}; c), and the degree of soil water repellency after 60˚C heat treatment (WR_{60}; d) for each application rate of GRF in Upernaviarsuk (UP) field. The same parameters for the South Igaliku (SI) field are shown in e–h. Capital letters denote significant groupings in the post-treatment results from the ANOVA and Holm-Sidak test, and asterisks denote significant differences between pre-sampling and post-treatment from the paired t-test (*$p < 0.05$, **$p < 0.01$, ***$p < 0.001$). Note that WR_{105} and WR_{60} are presented as 71.27-WR (mN m^{-1}), which represents the decrease in surface tension compared to pure H_2O to increase legibility. ANOVA, analysis of variance; WR-W curve, curve of water repellent soils.

that of the pre-GRF sampling campaign. In comparison, most GRF-treated samples were located below the regression line for WR_{AREA} (Figure 5a). Further, the WR_{AREA} measurements of the SI control samples were located above the regression line (Figure 5e), while the WR_{AREA} of GRF-treated samples were located below the regression line. Measurements of WR_{AREA} of the SI field were generally located at an increasing distance below the regression line with increasing amounts of added GRF. While these results only indicate that the OC becomes less potent in causing WR after GRF application, they highlight that the OC variability obscured the results in Figure 4a,e.

For W_{NON}, the trend was not as clear as for WR_{AREA}. However, most W_{NON} measurements of GRF-treated samples were located at or below the regression line for both fields (Figure 5b,f). The effect of the clay fraction on W_{NON} has been investigated in the paper of Weber et al. (2021). They found that clay content had an increasing effect on W_{NON} on Greenlandic soil samples (through multiple linear regression utilizing clay and OC content as predictors). Further, the study by Lichner et al. (2006) investigated clay amendment as a method for alleviating WR. In their study, clay amendment was also found to increase W_{NON} irrespective of the type of clay mineral added (illite, kaolinite, and montmorillonite).
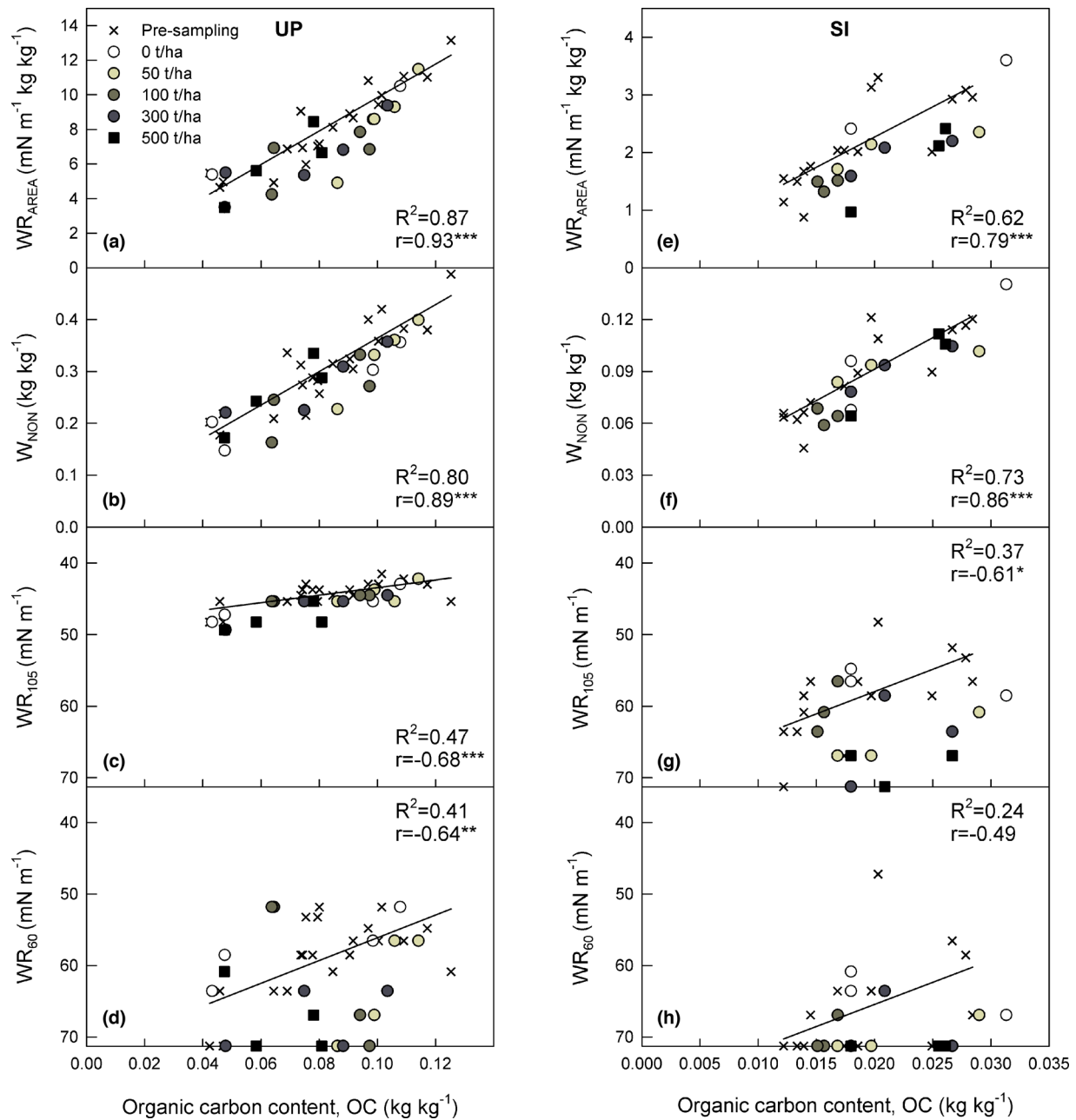
FIGURE 5 Scatter plots of the trapezoidal integrated area of the WR-W curve (WR$_{AREA}$; a), the critical water content (W$_{NON}$; b), the degree of soil water repellency after 105°C heat treatment (WR$_{105}$; c), and the degree of soil water repellency after 60°C heat treatment (WR$_{60}$; d) as a function of organic carbon content (OC) for the Upernaviarsuk (UP) field, and the same parameters for the South Igaliku (SI) field (e–h). The black crosses and their best linear relationship (black line) represent the baseline of the fields before the application of glacial rock flour (GRF). The coefficient of determination (R^2) and Pearson correlation coefficient (r) for each baseline is shown with asterisks denoting significant correlations (*$p < 0.05$, **$p < 0.01$, ***$p < 0.001$). WR-W curve, curve of water repellent soils.

Thus, variations in texture might interfere with the relations between WR and OC content since clay content can directly affect the soil water retention and thereby displace the entire WR-W curve along the x-axis (Figure 2). This intimate relationship between soil water retention and the WR-W was also highlighted in the study by Weber et al. (2021), who found that the slope of the dry-region soil water retention curve was the best single predictor of W$_{NON}$ for Greenlandic agricul-

tural soils. Weber et al. (2021) also noted that changes in clay content could also result in ambiguous effects on the WR$_{AREA}$, as increasing clay contents can increase the soil water retention (and thereby increase WR$_{AREA}$) while simultaneously resulting in lower degrees of WR across the WR-W curve.

The GRF treatments also affected the correlation between WR$_{60}$ and WR$_{105,}$ and OC, respectively (Figure 5c and d, g

and h). The majority of the post-GRF measurements of WR_{105} and WR_{60} were located close to or below the regression line. For WR_{105} of the UP field (Figure 5c), the three samples treated with 500 ton ha^{-1} GRF were less water repellent than the remaining samples when plotted against the respective OC contents. As discussed earlier, several GRF-treated SI samples became hydrophilic at WR_{60} and WR_{105}, while a hydrophilic state was achieved at WR_{60} for several UP samples.

3.4 | Normalization of WR_{AREA} to soil water retention

Soil water retention in the relatively dry end of the soil water retention curve is governed by the adsorption of water onto the surface area available from OC, clay, and fine silt content (Jensen et al., 2015; Karup et al., 2017). Therefore, some of the effects from GRF on WR-W curves can be masked by variabilities in fine minerals and OC content within and between the field plots. As mentioned, differences in clay content can affect the W_{NON}, since clay increases the soil's water-holding capacity and the W at a given pF value. This causes a displacement of the WR measurements when plotted against the W; a displacement that might not happen if soil water repellency measurements were plotted against pF-values. Thus, W_{NON} and WR_{AREA} are sensitive to variabilities in fine minerals and OC content. Kawamoto et al. (2007) plotted WR-W curves as a function of volumetric water content and pF values, respectively. The critical water content exhibited much less variability among the samples after conversion to pF, indicating that soil water retention has a normalizing effect on WR-W curves. Further, a recent study showed that WR was intimately linked to the water vapor isotherms of soils from Denmark and Greenland with an OC ranging from 0.014 to 0.369 kg kg^{-1} (Hermansen et al., 2021). Hermansen et al. (2021) were, among other things, able to predict WR_{AREA} and W_{NON} with high accuracy (R^2 of 0.98 and 0.97, respectively) from the water content at 50% relative humidity. Therefore, desorption isotherms were applied to normalize SWR_{AREA} to soil water retention. This was done by dividing the SWR_{AREA} with the negative inverse Campbell-Shiozawa slope, $-\alpha^{-1}$ (Campbell & Shiozawa, 1992) (Figure 6). This procedure, which is described in Section 2.5, was inspired by the findings of Weber et al. (2021), who found that $-\alpha^{-1}$ was markedly better than OC content at predicting the W_{NON} for 145 Greenlandic soil samples. The logical rationale was that both $-\alpha^{-1}$ (between 20% and 70% relative humidity) and the water content at 50% relative humidity are governed by the dry-region soil water retention, which also is strongly correlated to the specific surface area of the soil (Leão & Tuller, 2014; Resurreccion et al., 2011). The vapor sorption analyzer was chosen because it contains an internal high-precision scale, which enables the direct measurement of the
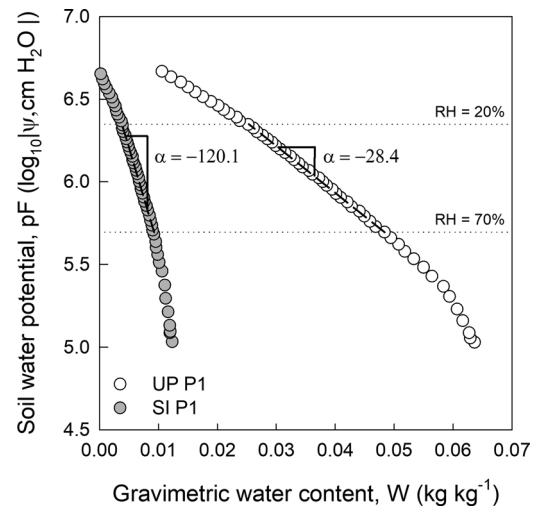

FIGURE 6 Conceptual plot detailing the desorption isotherm for one pre-treatment UP soil (white circle) and one pre-treatment SI soil (grey circle), and the linear regression of the Campbell-Shiozawa slopes (α) between 20% and 70% relative humidity (RH). SI, South Igaliku; UP, Upernaviarsuk.

$-\alpha^{-1}$, which circumvents the uncertainties associated with oven-drying soil.

The desorption isotherms exhibited a linear relationship between soil water potential (pF) and W in the range between 20% and 70% relative humidity (pF 6.35–5.69). Therefore, this pF-range was used to derive $-\alpha^{-1}$.

After normalization of WR_{AREA} with $-\alpha^{-1}$, the effect of GRF on WR was more evident (Figure 7). For the control treatment, the $WR_{AREA}/-\alpha^{-1}$ reached a higher level in the post-treatment samples than the pre-sampled samples for both the UP and SI fields, indicating a slight but non-significant increase in $WR_{AREA}/-\alpha^{-1}$ between the sampling years. However, the application of GRF lowered the $WR_{AREA}/-\alpha^{-1}$ such that the WR level became less after GRF treatment compared to the pre-sampling.

As shown in Figure 7, the relative reduction in $WR_{AREA}/-\alpha^{-1}$ is higher for the SI field than for the UP field at GRF application rates of 500 ton ha^{-1}. The higher effect of GRF on $WR_{AREA}/-\alpha^{-1}$ for the SI field might be caused by differences in texture and OC content between the fields. The soil across the SI field is generally lower in clay and OC contents than in the UP field. Thus, the GRF treatment implies a relatively higher increase in clay content for the SI field than for the UP field. Further, the OC content for the SI field is relatively low, meaning fewer hydrophobic surfaces need to be covered by clay minerals in the SI field compared to the UP field.

Overall, the normalization procedure looked promising, as the normalized WR_{AREA} values were comparable between the two fields, indicating that the approach can be used to compare WR across soils with different compositions and soil water retention.
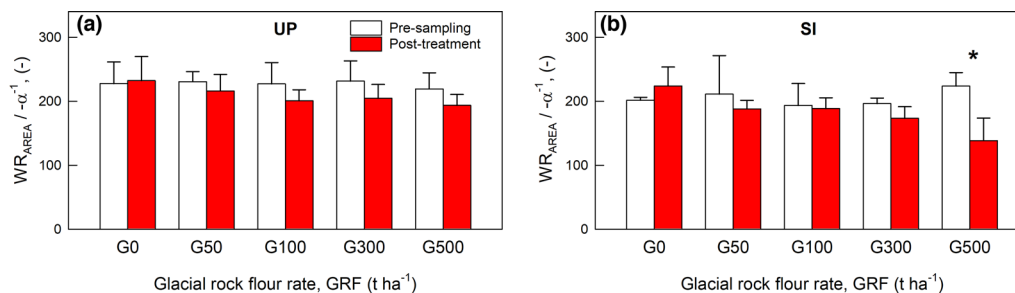
FIGURE 7 Bar charts of α-normalized WR_{AREA} for each application rate of GRF in UP (a) and SI (b). Asterisks denote a significant difference between pre-sampling and post-treatment from the paired t-test (*$p < 0.05$, **$p < 0.01$, ***$p < 0.001$). WR_{AREA}, the integrated trapezoidal area of the WR-W curve.

4 | CONCLUSION

This study provided the first investigation into the effects of GRF as a soil amendment for WR. The study was carried out in two randomized field experiments across two Greenlandic cultivated fields.

The bimodal WR versus W curves were affected by GRF treatments of 300 and 500 ton ha^{-1} because most curves became temporarily hydrophilic at the local minimum in WR around water contents corresponding to air-dry conditions. Further, a consistent decrease in all the investigated WR parameters (WR_{AREA}, W_{NON}, WR_{60}, and WR_{105}) was observed for the treatments with 300 and 500 ton ha^{-1}.

Regarding the relations between WR parameters and OC, the WR_{AREA} and W_{NON} from both fields exhibited relatively strong linear relations to OC. Overall, the treatments with GRF lowered the level of WR in relation to the corresponding OC content for all the investigated WR parameters. Still, variances in OC content and texture slightly masked the trends. Thus, normalization of the WR_{AREA} by soil water retention (utilization of the Campbell-Shiozawa slope) reduced the masking effect of varying OC content and texture on WR. The GRF treatment reduced the normalized WR_{AREA} across all treatment levels when compared to both the control plots and the same plot before GRF application, but the effects were only statistically significant at 500 ton ha^{-1} in the SI field.

While the results of the present study indicate that GRF application may be useful for reducing the WR of Greenlandic agricultural soils, further studies with a higher statistical power, less soil variability, and a longer time scale are needed to assess its effectiveness.

AUTHOR CONTRIBUTIONS
Peter Weber: Conceptualization; data curation; formal analysis; investigation; methodology; resources; visualization; writing—original draft; writing—review and editing. **Cecilie Hermansen**: Data curation; investigation; methodology; writing—original draft; writing—review and editing. **Charles Pesch**: Investigation; resources; writing—review and editing. **Per Møldrup**: Conceptualization; funding acquisition; supervision; writing—review and editing. **Mogens Greve**: Conceptualization; funding acquisition; investigation; resources; supervision; writing—review and editing. **Natasha Blaesbjerg**: Investigation; writing—review and editing. **Gabriela Moreno**: Formal analysis; investigation; writing—review and editing. **Emmanuel Arthur**: Data curation; investigation; methodology; writing—review and editing. **Lis de Jonge**: Conceptualization; funding acquisition; methodology; project administration; supervision; writing—review and editing.

CONFLICT OF INTEREST STATEMENT
The authors declare no conflicts of interest.

ORCID
Peter L. Weber https://orcid.org/0000-0001-9249-0796
Cecilie Hermansen https://orcid.org/0000-0002-1925-3732
Charles Pesch https://orcid.org/0000-0003-4120-0239
Mogens H. Greve https://orcid.org/0000-0001-9099-8940
Natasha H. Blaesbjerg https://orcid.org/0000-0001-8340-3590
Emmanuel Arthur https://orcid.org/0000-0002-0788-0712
Lis Wollesen de Jonge https://orcid.org/0000-0003-2874-0644

REFERENCES

Arthur, E., Tuller, M., Moldrup, P., & Wollesen de Jonge, L. (2014). Evaluation of a fully automated analyzer for rapid measurement of water vapor sorption isotherms for applications in soil science. *Soil Science Society of America Journal*, *78*, 754–760. https://doi.org/10.2136/sssaj2013.11.0481n

Asiaq Greenland Survey. (2022). *Greenland 1:250.000 grayscale [Geographic map]*. Asiaq Greenland Survey. https://en.nunagis.gl/

Bennike, O., Björck, S., & Lambeck, K. (2002). Estimates of South Greenland late-glacial ice limits from a new relative sea level curve. *Earth and Planetary Science Letters*, *197*, 171–186. https://doi.org/10.1016/S0012-821X(02)00478-8

Bisdom, E. B. A., Dekker, L. W., & Schoute, J. F. T. (1993). Water repellency of sieve fractions from sandy soils and relationships with organic material and soil structure. *Geoderma*, *56*, 105–118. https://doi.org/10.1016/0016-7061(93)90103-R

Blaesbjerg, N. H., Weber, P. L., de Jonge, L. W., Moldrup, P., Greve, M. H., Arthur, E., Knadel, M., & Hermansen, C. (2022). Water repellency prediction in high-organic Greenlandic soils: Comparing vis–NIRS to pedotransfer functions. *Soil Science Society of America Journal*, *86*(3),1–15. https://doi.org/10.1002/saj2.20407

Brown, M. B., & Forsythe, A. B. (1974). Robust tests for the equality of variances. *Journal of the American Statistical Association*, *69*, 364–367. https://doi.org/10.1080/01621459.1974.10482955

Campbell, G. S., & Shiozawa, S. (1992). Prediction of hydraulic properties of soils using particle-size distribution and bulk density data. In M. Th. van Genuchten, F. J. Leij, & L. J. Lund (Eds.), *Proceedings of the International Workshop on indirect Methods of Estimating the Hydraulic Properties of Unsaturated Soils* (pp. 317–328). US Salinity Lab.

Cann, M. A. (2000). Clay spreading on water repellent sands in the south east of South Australia promoting sustainable agriculture. *Journal of Hydrology*, *231*, 333–341. https://doi.org/10.1016/S0022-1694(00)00205-5

Cappelen, J. (2021). *Greenland-DMI historical climate data collection 1784–2020* (Report no. 21-04). Danish Meteorological Institute.

Caviezel, C., Hunziker, M., & Kuhn, N. (2017). Bequest of the Norseman—The potential for agricultural intensification and expansion in southern Greenland under climate change. *Land*, *6*, 87. https://doi.org/10.3390/land6040087

Christensen, J. H., Olesen, M., Boberg, F., Stendel, M., & Koldtoft, I. (2016). *Fremtidige klimaforandringer i Grønland: Kujalleq Kommune* [Report no. 15-04 (1/6)]. Danish Meterological Institute.

de Jonge, L. W., Jacobsen, O. H., & Moldrup, P. (1999). Soil water repellency: Effects of water content, temperature, and particle size. *Soil Science Society of America Journal*, *63*, 437–442. https://doi.org/10.2136/sssaj1999.03615995006300030003x

de Jonge, L. W., Moldrup, P., & Jacobsen, O. H. (2007). Soil-water content dependency of water repellency in soils: Effect of crop type, soil management, and physical-chemical parameters. *Soil Science*, *172*, 577–588. https://doi.org/10.1097/SS.0b013e318065c090

Diamantis, V., Pagorogon, L., Gazani, E., Gkiougkis, I., Pechtelidis, A., Pliakas, F., van den Elsen, E., Doerr, S. H., & Ritsema, C. J. (2017). Use of clay dispersed in water for decreasing soil water repellency. *Land Degradation and Development*, *28*, 328–334. https://doi.org/10.1002/ldr.2600

Dlapa, P., Doerr, S. H., Lichner, L., Šír, M., & Tesař, M. (2004). Alleviation of soil water repellency: Effect of kaolinite and Ca-montmorillonite. *Plant, Soil and Environment*, *49*, 358–363. https://doi.org/10.17221/4044-PSE

Doerr, S. H., Shakesby, R. A., & Walsh, R. P. D. (2000). Soil water repellency: Its causes, characteristics and hydro-geomorphological significance. *Earth Science Reviews*, *51*, 33–65. https://doi.org/10.1016/S0012-8252(00)00011-8

Fu, Z., Hu, W., Beare, M. H., Müller, K., Wallace, D., & Chau, H. W. (2021). Contributions of soil organic carbon to soil water repellency persistence: Characterization and modelling. *Geoderma*, *401*, 115312. https://doi.org/10.1016/j.geoderma.2021.115312

Gee, G. W., & Or, D. (2002). Particle-size analysis. In J. H. Dane & G. C. Topp (Eds.), *Methods of soil analysis, Part 4: Physical methods* (pp. 255–293). ASA and SSSA.

Hallett, P. D. (2008). A brief overview of the causes, impacts and amelioration of soil water repellency—A review. *Soil and Water Research*, *3*, 21–29. https://doi.org/10.17221/1198-swr

Hermansen, C., Moldrup, P., Müller, K., Jensen, P. W., van den Dijssel, C., Jeyakumar, P., & de Jonge, L. W. (2019). Organic carbon content controls the severity of water repellency and the critical moisture level across New Zealand pasture soils. *Geoderma*, *338*, 281–290. https://doi.org/10.1016/j.geoderma.2018.12.007

Hermansen, C., Norgaard, T., de Jonge, L. W., Weber, P. L., Moldrup, P., Greve, M. H., Tuller, M., & Arthur, E. (2021). Linking water vapor sorption to water repellency in soils with high organic carbon contents. *Soil Science Society of America Journal*, *85*, 1037–1049. https://doi.org/10.1002/saj2.20248

Holm, S. (1979). A simple sequentially rejective multiple test procedure. *Scandinavian Journal of Statistics*, *6*, 65–70.

IUSS Working Group WRB. (2014). *World reference base for soil resources 2014. International soil classification system for naming soils and creating legends for soil maps* (Report No. 106). FAO.

Jacobsen, N. K. (1987). Studies on soils and potential for soil erosion in the sheep farming area of South Greenland. *Arctic and Alpine Research*, *19*, 498–507. https://doi.org/10.2307/1551416

Jensen, D. K., Tuller, M., de Jonge, L. W., Arthur, E., & Moldrup, P. (2015). A new two-stage approach to predicting the soil water characteristic from saturation to oven-dryness. *Journal of Hydrology*, *521*, 498–507. https://doi.org/10.1016/j.jhydrol.2014.12.018

Karup, D., Moldrup, P., Tuller, M., Arthur, E., & de Jonge, L. W. (2017). Prediction of the soil water retention curve for structured soil from saturation to oven-dryness. *European Journal of Soil Science*, *68*, 57–65. https://doi.org/10.1111/ejss.12401

Kawamoto, K., Moldrup, P., Komatsu, T., de Jonge, L. W., & Oda, M. (2007). Water repellency of aggregate size fractions of a volcanic ash soil. *Soil Science Society of America Journal*, *71*, 1658–1666. https://doi.org/10.2136/sssaj2006.0284

Kercheva, M., Ivanov, P., Dimitrov, E., Banov, M., & Atanassova, I. (2021). Soil water repellency characteristic curve of Spolic Technosols from the region of Maritsa-Iztok coal mine in Bulgaria. *Geoderma Regional*, *26*. https://doi.org/10.1016/j.geodrs.2021.e00416

King, P. M. (1981). Comparison of methods for measuring severity of water repellence of sandy soils and assessment of some factors that affect its measurement. *Australian Journal of Soil Research*, *19*, 275–285. https://doi.org/10.1071/SR9810275

Kokfelt, F. T., Weng, L. W., & Willerslev, E. (2019). *Geological map of South and South West Greenland—1:100000*. Geological Survey of Denmark and Greenland (GEUS).

Leão, T. P., & Tuller, M. (2014). Relating soil specific surface area, water film thickness, and water vapor adsorption. *Water Resources Research*, *50*, 7873–7885. https://doi.org/10.1002/2013WR014941

Lichner, L., Dlapa, P., Doerr, S. H., & Mataix-Solera, J. (2006). Evaluation of different clay minerals as additives for soil water repellency alleviation. *Applied Clay Science*, *31*, 238–248. https://doi.org/10.1016/j.clay.2005.10.012

Ma'Shum, M., Oades, J. M., & Tate, M. E. (1989). The use of dispersible clays to reduce water-repellency of sandy soils. *Australian Journal of Soil Research*, *27*, 797–806. https://doi.org/10.1071/SR9890797

McKissock, I., Gilkes, R. J., & Walker, E. L. (2002). The reduction of water repellency by added clay is influenced by clay and soil properties. *Applied Clay Science*, *20*, 225–241. https://doi.org/10.1016/S0169-1317(01)00074-6

Müller, K., & Deurer, M. (2011). Review of the remediation strategies for soil water repellency. *Agriculture, Ecosystems and Environment*, *144*, 208–221. https://doi.org/10.1016/j.agee.2011.08.008

Müller, K., Deurer, M., Slay, M., Aslam, T., Carter, J. A., & Clothier, B. E. (2010). Environmental and economic consequences of soil water repellency under pasture. *Proceedings of the New Zealand Grassland Association*, *72*, 207–210. https://doi.org/10.33584/jnzg.2010.72.2786

Pesch, C., Weber, P. L., Moldrup, P., Jonge, L. W., Arthur, E., & Greve, M. H. (2022). Physical characterization of glacial rock flours from fjord deposits in South Greenland—Toward soil amendment. *Soil Science Society of America Journal*, *86*, 407–422. https://doi.org/10.1002/saj2.20352

Regalado, C. M., Ritter, A., De Jonge, L. W., Kawamoto, K., Komatsu, T., & Moldrup, P. (2008). Useful soil-water repellency indices: Linear correlations. *Soil Science*, *173*, 747–757. https://doi.org/10.1097/SS.0b013e31818d4163

Resurreccion, A. C., Moldrup, P., Tuller, M., Ferré, T. P. A., Kawamoto, K., Komatsu, T., & de Jonge, L. W. (2011). Relationship between specific surface area and the dry end of the water retention curve for soils with varying clay and organic carbon contents. *Water Resources Research*, *47*, W06522. https://doi.org/10.1029/2010WR010229

Roper, M. M., Davies, S. L., Blackwell, P. S., Hall, D. J. M., Bakker, D. M., Jongepier, R., & Ward, P. R. (2015). Management options for water-repellent soils in Australian dryland agriculture. *Soil Research*, *53*, 786–806. https://doi.org/10.1071/SR14330

Roy, J. L., & McGill, W. B. (2002). Assessing soil water repellency using the molarity of ethanol droplet (MED) test. *Soil Science*, *167*, 83–97. https://doi.org/10.1097/00010694-200202000-00001

Seaton, F. M., Jones, D. L., Creer, S., George, P. B. L., Smart, S. M., Lebron, I., Barrett, G., Emmett, B. A., & Robinson, D. A. (2019). Plant and soil communities are associated with the response of soil water repellency to environmental stress. *Science of The Total Environment*, *687*, 929–938. https://doi.org/10.1016/j.scitotenv.2019.06.052

Shapiro, S. S., & Wilk, M. B. (1965). An analysis of variance test for normality (complete samples). *Biometrika*, *52*, 591–611. https://doi.org/10.1093/biomet/52.3-4.591

Soil Survey Staff. (1999). *A basic system of soil classification for making and interpreting soil surveys* (Agricultural Handbook 436). USDA Natural Resources Conservation Service.

Sukstorf, F. N., Bennike, O., & Elberling, B. (2020). Glacial rock flour as soil amendment in subarctic farming in South Greenland. *Land*, *9*, 198. https://doi.org/10.3390/land9060198

Wallis, M. G., & Horne, D. J. (1992). Soil water repellency. In B. A. Stewart (ed.), *Advances in soil science* (Vol. 20, pp. 91–144). Springer. https://doi.org/10.1007/978-1-4612-2930-8_2

Ward, P. R., & Oades, J. M. (1993). Effect of clay mineralogy and exchangeable cations on water-repellency in clay-amended sandy soils. *Australian Journal of Soil Research*, *31*, 351–364. https://doi.org/10.1071/SR9930351

Weber, P. L., de Jonge, L. W., Greve, M. H., Norgaard, T., & Moldrup, P. (2020). Gas diffusion characteristics of agricultural soils from South Greenland. *Soil Science Society of America Journal*, *84*, 1606–1619. https://doi.org/10.1002/saj2.20114

Weber, P. L., Hermansen, C., Norgaard, T., Pesch, C., Moldrup, P., Greve, M. H., Müller, K., Arthur, E., & de Jonge, L. W. (2021). Moisture-dependent water repellency of Greenlandic cultivated soils. *Geoderma*, *402*. https://doi.org/10.1016/j.geoderma.2021.115189

Wijewardana, N. S., Müller, K., Moldrup, P., Clothier, B., Komatsu, T., Hiradate, S., de Jonge, L. W., & Kawamoto, K. (2016). Soil-water repellency characteristic curves for soil profiles with organic carbon gradients. *Geoderma*, *264*, 150–159. https://doi.org/10.1016/j.geoderma.2015.10.020